

Order and Chaos in the Local Disc Stellar Kinematics

R. Fux

*Research School of Astronomy and Astrophysics, Mount Stromlo
 Observatory, Canberra, Australia*

Abstract. The effects of the Galactic bar on the velocity distribution of old disc stars in the Solar neighbourhood are investigated using high-resolution 2D test particle simulations. A detailed orbital analysis reveals that the structure of the $U - V$ distribution in these simulations is closely related to the phase-space extent of regular and chaotic orbits. At low angular momentum and for a sufficiently strong bar, stars mainly follow chaotic orbits which may cross the corotation radius and the $U - V$ contours follow lines of constant Jacobi's integral except near the regions occupied by weakly populated eccentric regular orbits. These properties can naturally account for the observed outward motion of the local high asymmetric drift stars.

1. Introduction

The observed local stellar velocity distribution in the $U - V$ plane, where U is the radial velocity positive towards the anti-centre and V the azimuthal velocity positive towards galactic rotation, betrays a large stream of old disc stars with an asymmetric drift $S \approx 40 - 50 \text{ km s}^{-1}$ and $\overline{U} > 0$ (e.g. Dehnen 1998), which hereafter will be referred to as the ‘‘Herculis’’ stream according to a co-moving Eggen group. One of the most reasonable interpretation of this stream relies on the influence of the Galactic bar, which is believed to have a corotation radius $R_{\text{CR}} \approx 3.5 - 5 \text{ kpc}$ and a major-axis presently leading by $\varphi \approx 15^\circ - 45^\circ$ the Sun's azimuth. Raboud et al. (1998) have shown that N -body models of the Milky Way do produce a mean outward motion of disc particles at realistic positions for the Sun relative to the bar and suggest that the Herculis stream involves stars on hot orbits, i.e. orbits with a high enough value of Jacobi's integral to cross the corotation radius, whereas Dehnen (2000, hereafter D2000) relates this velocity mode and the main low-asymmetric drift mode of the observed $U - V$ distribution to the coexistence near the outer Lindblad resonance (OLR) of the inner anti-bar and outer bar elongated periodic orbits replacing the circular orbit close to the OLR in a rotating barred potential (i.e. the same idea introduced by Kalnajs 1991 to explain the Hyades and Sirius streams), and attributes the valley at $S \approx 30 \text{ km s}^{-1}$ between the two modes (respectively ‘‘OLR’’ and ‘‘LSR’’ mode in his terminology) to stars on unstable OLR orbits. This paper analyses the role of bar induced chaotic orbits in this context and confronts both alternatives using a similar 2D modelling technique as in Dehnen's work. The details are presented in Fux (2000).

2. Resonances and periodic orbits

The working potential is the same as in D2000, consisting of the sum of an axisymmetric logarithmic potential with constant circular velocity V_o and of a rotating quadrupole term with a bar strength $F = 0.15$, where F is defined as the maximum azimuthal force on the circle passing through the ends of the bar normalised by the axisymmetric radial force at same radius ($F = 8.89\alpha$ in Dehnen's notation). The position in space will be parametrised by the galactocentric distance relative to the OLR radius $R_{\text{OLR}} = (1 + 1/\sqrt{2})R_{\text{CR}}$ and the angle φ relative to the major axis of bar. A distance of $R/R_{\text{OLR}} = 1.1$ implies $R_{\text{CR}} = 4.26$ kpc if $R = R_o = 8$ kpc.

Figure 1 (left) shows the characteristic curves in the Hamiltonian– x plane (at $y = 0$ and $\dot{y} > 0$) of the main periodic orbits existing near the OLR and closing after one rotation in the rotating frame, using the labelling of Contopoulos & Grosbol (1989). The curves essentially resemble those of the circular orbit and of the resonant orbits in the axisymmetric limit, except near the resonances of the circular orbit where bifurcations may transform into gaps, as is the case at the OLR (e.g. Sellwood & Wilkinson 1993). Figure 1 also displays some members of the $x_1(1)$ and $x_1(2)$ families. The thick orbits are examples of the perpendicularly oriented orbits that replace the circular orbit near the OLR and which are responsible for the bimodality in the observed $U - V$ distribution according to D2000. In both families, the orbits develop loops at high eccentricity, i.e. on the part of the characteristic curves emerging leftwards from the zero velocity curve and where $\dot{x} \neq 0$, and the $x_1(1)$ orbits are stable over a remarkable eccentricity range. Figure 2 shows the location in the $U - V$ plane of the $-4/1$, $-2/1$ (OLR) and $-1/1$ resonances in the axisymmetric part of the potential for different space positions, and of the periodic orbits passing through these positions in the total axisymmetric+bar potential. At $\varphi = 90^\circ$ most resonant periodic orbits are stable, except for instance the $x_1^*(2)$ orbit at $R/R_{\text{OLR}} \gtrsim 1.1$, whereas at $\varphi = 0$, most of them are unstable.

3. Hot orbits

In a rotating barred potential, the value of the Hamiltonian $H = \frac{1}{2}\dot{\vec{x}}^2 + \Phi_{\text{eff}}(\vec{x})$, where $\Phi_{\text{eff}}(\vec{x})$ is the effective potential, is the only classical integral of motion, known as Jacobi's integral. Two critical values of this integral are related to the Lagrangian points $L_{1/2}$ and $L_{4/5}$, i.e. respectively the saddle points and maxima of $\Phi_{\text{eff}}(\vec{x})$. If $H > H_{12} \equiv \Phi_{\text{eff}}(L_{1/2})$, an orbit is susceptible to cross the corotation radius, defining the *hot orbit* category, and if $H > H_{45} \equiv \Phi_{\text{eff}}(L_{4/5})$, an orbit is no longer spatially confined by this integral.

If U and V are measured relative to the galactic centre, the contours of constant H in the $U - V$ plane are circles centred on $(V, U) = (R\Omega_{\text{P}}, 0)$, where Ω_{P} is the pattern speed of the bar, and of radius $\sqrt{2(H - \Phi_{\text{eff}})}$. Figure 2 gives the H_{12} and H_{45} contours as a function of space position for the working potential. The hot orbits are those outside (low V) the former contour. At $R = R_{\text{OLR}}$ and $\varphi = 30^\circ$, the H_{12} contour crosses the V -axis at $S = V_o - V \approx 0.177V_o = 35 \text{ km s}^{-1}$ for $V_o = 200 \text{ km s}^{-1}$, placing the Hercules stream in the hot orbit zone.

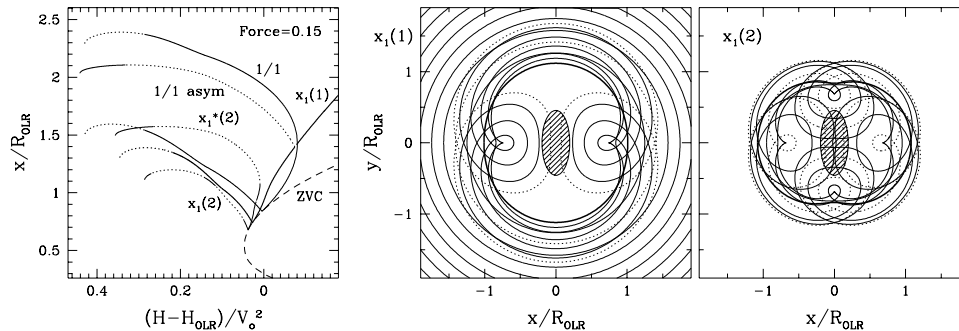


Figure 1. Left: characteristic diagram of the relevant periodic orbit families for $F = 0.15$. The dashed line indicates the zero velocity curve and H_{OLR} is the Hamiltonian of the circular orbit at the OLR in the axisymmetric part of the potential. Middle and right: sequences of $x_1(1)$ and $x_1(2)$ orbits, with the thick line representing the orbit of lowest apocentre and of lowest Hamiltonian respectively. The orientation of the bar is sketched by the shaded ellipse. In all frames, full and dotted lines stand for stable and unstable orbits respectively.

4. Regular and chaotic regions of phase-space

The next step after the periodic and hot orbits is to determine the extension in phase-space of the regular orbits trapped around the stable periodic orbits and of the chaotic regions. A convenient tool for this purpose are the Liapunov exponents, which describe the mean exponential rate of divergence of two trajectories with infinitesimally different initial conditions. The largest such exponent, λ_1 , determines the degree of stochasticity of the orbits and vanishes for regular orbits. Figure 2 gives the divergence timescale $t_\lambda \equiv 1/\lambda_1$ of the orbits as a function of planar velocity and space position.

The Liapunov divergence timescale can be as low as a few orbital times for chaotic orbits. As expected, the stable periodic orbits always lie within regular regions and the unstable orbits within chaotic regions. Furthermore, the H_{12} contour appears as the average transition from regular motion at low H to chaotic motion at high H , and thus most hot orbits are chaotic. Due to the four-fold symmetry of the potential, the diagrams at $\varphi = 0$ and $\varphi = 90^\circ$ are symmetric with respect to $U = 0$, and more generally, diagrams at supplementary angles are anti-symmetric to each other in U . At $\varphi = 90^\circ$, the $-2/1$ and $-1/1$ resonance curves are mainly embedded within broad arcs of regular orbits spaced by chaotic regions at large H , while at $\varphi = 0$, these regular arcs occur between the resonance curves. At intermediate angles, the regular and chaotic regions become offset from the resonance curves and the U -symmetry brakes. In particular, for $\varphi \sim 30^\circ$ and for the displayed radial range, a prominent region of regular orbits trapped around stable eccentric $x_1(1)$ orbits extends down to negative U , bounded roughly by the OLR curve on the right and penetrating well inside the hot orbit zone, whereas the positive U part of the OLR curve is surrounded by a wide chaotic region extending somewhat inside the H_{12} contour and coinciding very well with the observed $U - V$ location of the Hercules

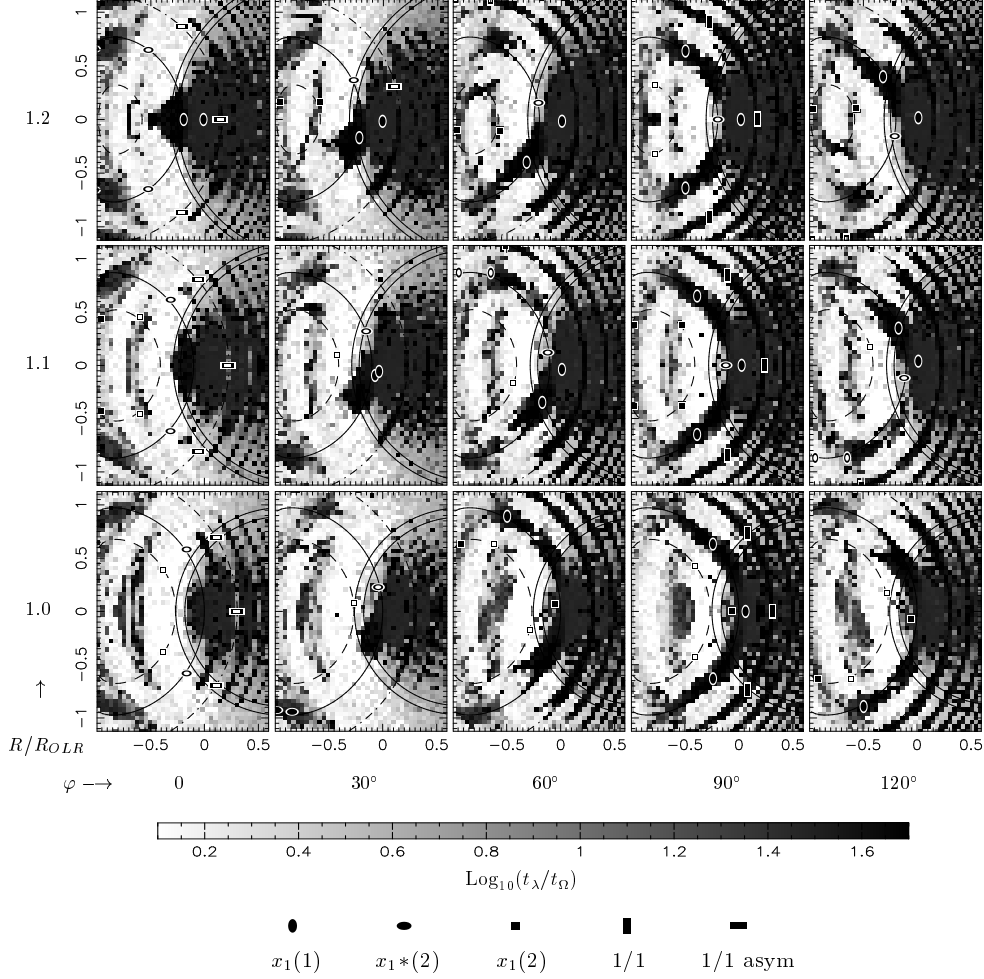


Figure 2. Liapunov divergence timescale of the orbits in the $U - V$ plane as a function of space position, for $F = 0.15$. The horizontal and vertical axes of each frame are V/V_0 and U/V_0 respectively, with the origin at the circular orbit of the underlying axisymmetric potential. The timescale is in units of local circular period t_Ω . The dark and white regions respectively indicate regular and chaotic orbits, the various full and empty symbols the stable and unstable periodic orbits, the circular arcs open towards the right the H_{12} and H_{45} contours, and the dash-dotted, solid and dashed curves the $-1/1$, $-2/1$ and $-4/1$ resonances in the axisymmetric part of the potential.

stream. Note that since 2D axisymmetric potentials are always integrable, all chaotic regions reported here owe uniquely to the bar.

A detailed investigation reveals that the regular orbits associated with the stable low eccentricity periodic orbits of the $x_1(2)$ family exist for $R/R_{OLR} \lesssim 1.1$ and over an angle range around $\varphi = 90^\circ$ increasing as R decreases. Elsewhere, unstable $x_1^*(2)$ orbits have completely substituted to the regular $x_1(2)$ islands.

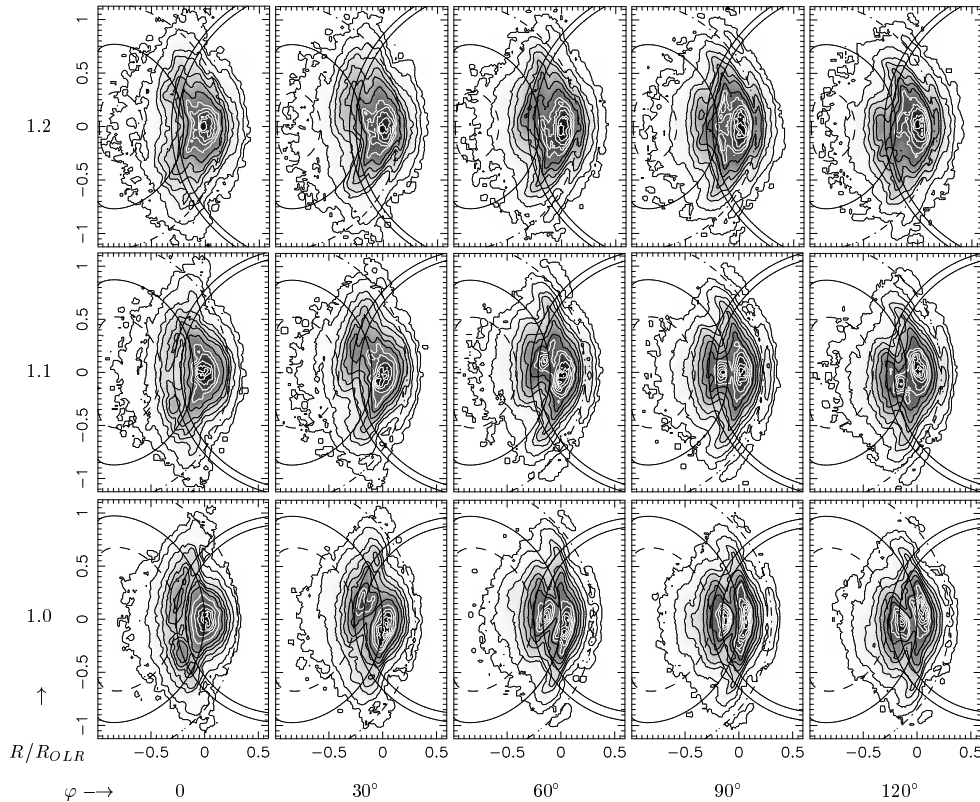


Figure 3. Velocity distribution as a function of bar parameters in the test particle simulations with $F = 0.15$. The distributions are averaged over the time interval going from 55 to 65 bar rotations. The axes of the frames and the resonance and H contours are as in Figure 2.

In particular, there is no $x_1(2)$ streaming motion expected at $R/R_{OLR} = 1.1$ and $\varphi = 30^\circ$ in the present working potential.

5. Phase-space crowding

Finally, we want to know how nature populates the available orbits. This is done by test particle simulations starting with exactly the same initial axisymmetric distribution functions f_o and growing the bar the same way (i.e. over 2 bar rotations) as in Dehnen's default simulations. However, we do not apply the claimed high-resolution and noise-free backward integration technique based on the conservation of the phase-space density along orbits. The reason is because much longer integration times than the few bar rotations adopted in D2000 are necessary to get phase-mixed and quasi-steady evolved distribution functions, and that for integration times larger than about 10 bar rotations, the fine-grained $U - V$ distributions resulting from this technique become highly fluctuating on small scales and even noisy in the chaotic regions and thus must be smoothed to yield the physical coarse-grained distributions. Therefore, we decided to use

the standard forward integration technique, sampling f_o with $N = 10^6$ particles, and to average the velocity distributions, derived within finite volumes of radius $R/80$, over 10 bar rotations to improve the statistics and also to minimise the phase-mixing problem. The results are depicted in Figure 3. Here the distance parameters in f_o always scale as R and the truly changing parameters are those of the bar. Hence frames at different R/R_{OLR} come from distinct simulations.

The $U - V$ distributions seem to present the same symmetry properties in U as described in the previous section for the Liapunov divergence timescale. This is obviously not the case in D2000, as a consequence of the too short integration. The high angular momentum peak of the velocity distributions also coincides better with the trace of the non-resonant $x_1(1)$ orbits at $U = 0$. The regular low eccentricity $x_1(2)$ regions also produce a peak in the velocity distributions, which always lies inside the H_{12} contour.

In the hot orbit zone, the chaotic regions appear to be more heavily crowded than the regular regions. This is because the phase-space density in regular regions remains roughly constant during the simulations, whereas there is a net migration of particles on hot chaotic orbits from the inner to the outer space regions, and because the chaotic and regular regions are decoupled from each other, i.e. chaotic orbits cannot visit the regions occupied by regular orbits and vice versa. Hence at large H , the velocity distributions are dominated by chaotic orbits which are forced to avoid less populated regular regions. In the parameter range considered here, these forbidden regions are essentially the broad regular orbit regions around the stable eccentric $x_1(1)$ orbits. In particular, at $R/R_{\text{OLR}} = 1.1$ and $\varphi = 30^\circ$, this $x_1(1)$ region lies at $U \lesssim 0$, as mentioned above, and thus the main overdensity of hot chaotic orbits occurs at positive U , providing a natural interpretation of the Hercules stream. The depression on the right of this stream may be attributed to the decline of the hot orbit population as $H \rightarrow H_{12}$. The high eccentricity $x_1(1)$ region is part of Dehnen's valley, but represents *regular* OLR orbits, and the unstable $x_1^*(2)$ orbit does not always fall within this valley (e.g. at $R/R_{\text{OLR}} = 1.2$ and $\varphi = 30^\circ$).

Another property of the hot chaotic regions is that the contours of the velocity distribution follow the lines of constant Hamiltonian. This can be understood in terms of the Jeans theorem (see also the answer to Dehnen's question): in two-dimensions, chaotic orbits have no other integral of motion than Jacobi's integral and thus the distribution function in their neighbourhood depends only on this integral, i.e. on the value of the Hamiltonian.

References

- Contopoulos G., Grosbol P. 1989, A&AR 1, 261
- Dehnen W. 1998, AJ 115, 2384
- Dehnen W. 2000, AJ 119, 800 (D2000)
- Fux R. 2000, A&A in preparation
- Kalnajs A.J. 1991. In: Sundelius B. (ed.) Proc. Varberg Conf., Dynamics of Disc Galaxies. Göteborg, p. 323
- Raboud D., Grenon M., Martinet L., Fux R., Udry S. 1998, A&A 335, L61
- Sellwood J.A., Wilkinson A. 1993, Rep. Prog. Phys. 56, 173

Questions

Ortwin Gerhard: The spiral arms outside the Milky Way's bar region must modify the population seen in the $U - V$ diagram. Could you say how?

Roger Fux: The effect of spiral arms is not yet very clear. As evolving transient features, they certainly introduce a time dependency of the $U - V$ distributions and probably increase the amount of chaos. Since Jacobi's integral is then no longer conserved, they may also introduce some diffusion from the regular regions to the chaotic regions and vice versa (and the same remark is true for massive compact objects like giant molecular clouds). N -body simulations displaying spiral arms reveal time averaged $U - V$ distributions that are qualitatively similar to those of the test particle simulations presented here, but with an azimuthal phase shift apparently related to the twist of the potential well induced by the spiral arms outside the bar.

Walter Dehnen: How can stars stay on chaotic orbits, which due to their H are not bound to the galaxy?

Roger Fux: The timescale for chaotic hot orbits with moderate H to escape the galaxy is much larger than the orbital timescale and even the Hubble time (see for instance Kaufmann & Contopoulos 1996, A&A 309, 381). In particular, once phase-mixed, the distribution function in the neighbourhood of such orbits may be considered as almost steady, which is a necessary condition to apply the Jeans theorem.